Life Sciences 251 (2020) 117587

Contents lists available at ScienceDirect

Life Sciences

journal homepage: www.elsevier.com/locate/lifescie

Insulin-producing cells from mesenchymal stromal cells: Protection against cognitive impairment in diabetic rats depends upon implant site

Krista Minéia Wartchow[a], Leticia Rodrigues[a], Lílian Juliana Lissner[a], Barbara Carolina Federhen[a], Nicholas Guerini Selistre[a], Aline Moreira[a], Carlos-Alberto Gonçalves[a,*], Patrícia Sesterheim[b]

[a] Federal University of Rio Grande do Sul (UFRGS), Biochemistry Post-Graduate Program, Porto Alegre, Brazil
[b] Institute of Cardiology of Rio Grande do Sul, Experimental Center, Porto Alegre, Brazil

ARTICLE INFO

Keywords:
Diabetes mellitus
Hippocampus
Insulin-producing cells
MSCs
Subcutaneous implant
Cognitive impairment

ABSTRACT

Diabetes mellitus (DM) is a serious public health problem and can cause long-term damage to the brain, resulting in cognitive impairment in these patients. Insulin therapy for type 1 DM (DM1) can achieve overall blood glucose control, but glycemic variations can occur during injection intervals, which may contribute to some complications. Among the additional therapies available for DM1 treatment is the implantation of insulin-producing cells (IPCs) to attenuate hyperglycemia and even reverse diabetes. Here, we studied the strategy of implanting IPCs obtained from mesenchymal stromal cells (MSCs) from adipose tissue, comparing two different IPC implant sites, subcapsular renal (SR) and subcutaneous (SC), to investigate their putative protection against hippocampal damage, induced by STZ, in a rat DM1 model. Both implants improved hyperglycemia and reduced the serum content of advanced-glycated end products in diabetic rats, but serum insulin was not observed in the SC group. The SC-implanted group demonstrated ameliorated cognitive impairment (evaluated by novel object recognition) and modulation of hippocampal astroglial reactivity (evaluated by S100B and GFAP). Using GFP + cell implants, the survival of cells at the implant sites was confirmed, as well as their migration to the pancreas and hippocampus. The presence of undifferentiated MSCs in our IPC preparation may explain the peripheral reduction in AGEs and subsequent cognitive impairment recovery, mediated by autophagic depuration and immunomodulation at the hippocampus, respectively. Together, these data reinforce the importance of MSCs for use in neuroprotective strategies, and highlight the logistic importance of the subcutaneous route for their administration.

1. Introduction

Diabetes mellitus (DM) is a serious and growing public health problem, affecting around 30 million people of all ages. According to the American Diabetes Association, type 1 diabetes (DM1) accounts for 5 to 10% of the total diabetic population [19]. DM1 is a metabolic disorder, characterized by hyperglycemia caused by T cells infiltrated in the Langerhans islets, resulting in destruction of the pancreatic β-cells [6] and consequent loss of the production and secretion of insulin [9]. In Brazil, almost 90% of DM1 patients fail to achieve glycemic control [13].

In addition to the well-known peripheral complications resulting from DM, several studies report that the disease can also affect the central nervous system (CNS), incurring complications such as diabetic encephalopathy, and increasing the probability of cognitive decline and the acceleration of Alzheimer's disease (AD), among other dementias [4,31,37,88]. Experimental data in animal models of DM1, induced by streptozotocin (STZ), suggest that learning deficits resulting from DM are associated with impairments in synaptic plasticity in the hippocampus [49,84]. Through this model, a series of studies has demonstrated evidence of brain damage, including astrocyte reactivity [30,49], neuronal damage and memory deficits [46], and even deposition of β-amyloid peptide, in these rats [83].

Potential definitive treatment strategies for DM1, which intend to correct insulin dependence, include pancreas transplantation, pancreatic islet transplantation and, more recently, autoimmunity blockade and stem cell-based therapy [1,75]. Mesenchymal stromal cells (MSCs) can be obtained from various tissues for differentiation into insulin-producing cells (IPCs) [34,61,69,72,77]. The adipose tissue offers distinct advantages due to its availability and significant therapeutic

* Corresponding author at: Federal University of Rio Grande do Sul (UFRGS), Biochemistry Post-Graduate Program, Ramiro Barcelos, 2600-Anexo 90035003, Porto Alegre, RS, Brazil.
E-mail address: casg@ufrgs.br (C.-A. Gonçalves).

https://doi.org/10.1016/j.lfs.2020.117587
Received 20 January 2020; Received in revised form 21 March 2020; Accepted 22 March 2020
Available online 26 March 2020
0024-3205/

potential, characterized by its intrinsic regenerative capacity and its immunomodulatory properties [11,67]. The rate of adipose stromal cell (ADSC) isolation is 100% and the yield of adipose tissue is 40 times higher than that of bone marrow [35]. Therefore, in addition to being easily obtained, the adipose tissue is a rich source of stromal cells that can be successfully used in autologous transplants [45].

For regenerative application, the route for cell implantation is very important for the prediction of homing. Numerous sites have been proposed and tested, both experimentally and in some cases clinically, including the liver, the subcapsular region of the kidney, spleen, pancreas, omentum, gastrointestinal wall and subcutaneous spaces [40,47]. For some time, the kidney capsule was used for experimental islet implants [70]. This site offers many advantages, such as a highly vascularized space that provides better survival and graft protection [20,68]. Another attractive option for the implant is the subcutaneous site, which offers accessibility and retrievability, as well as the potential for biopsy and simple monitoring [8]. Nevertheless, it is still unclear as to what degree the implantation site influences the transplant outcome, and few studies have compared whether the IPC implantation site interferes in the cognitive deficit consequent to DM1.

Despite the successful transdifferentiation of ADSCs to IPCs, an ideal site for IPC transplantation has yet to be determined. To evaluate this issue, we investigated and compared the efficacy of IPC implants in the renal subcapsular space and subcutaneous region of rats submitted to the DM1 model induced by STZ. We looked at metabolic peripheral changes, as well as CNS alterations, particularly in the hippocampus, and observed cognitive behavior that is dependent on this brain region.

2. Material and methods

2.1. Animals

Eight-week-old male Wistar Kyoto rats (WKY) were used for mesenchymal stromal cell isolation from adipose tissue. Cells were then expanded and differentiated into insulin-producing cells (Institute of Cardiology of Rio Grande do Sul, Experimental Cardiology Center, Porto Alegre, Brazil). The animals were maintained in a constant 12-h light/dark cycle, at a temperature of 24 ± 2 °C, and 50–60% relative humidity, and were housed in groups of four in standard cages with ad libitum access to drinking water and standard food pellets. All animal procedures were performed according to guidelines of the National Institutes of Health Guide for the Care and Use of Laboratory Animals, and all protocols were approved by the Federal University of Rio Grande do Sul Animal Care and Use Committee (process number 30626). For MSC/IPC tracking, we used Lewis rats and transgenic (tg) Lewis rats ubiquitously expressing green fluorescent protein (GFP-tg Lewis).

2.2. Chemicals

Streptozotocin (STZ), fetal bovine serum (FBS), Dulbecco's modified Eagle medium (DMEM) and other materials for cell culture were purchased from Gibco BRL (Carlbad, CA, USA). S100B protein, anti-S100B antibody (SH-B1), *o*-phenylenediamine (OPD), anti-S100B antibody (clone SH-B) and anti-synaptophysin were purchased from Santa Cruz Biotechnology (Santa Cruz CA, USA). Anti-β-actin was from EMD Millipore (Darmstadt, Germany). Other reagents were purchased from local commercial suppliers (Sulquímica and Labsul, Porto Alegre, Brazil).

2.3. Isolation and expansion of adipose-derived mesenchymal stromal cells (ADSCs)

Epididymal fat was collected aseptically from WKY rats (or GFP-tg Lewis) and minced into small pieces. The fragments were digested with 1.5 mg/mL of collagenase type I (Sigma) and diluted in DMEM without serum for 20 min at 37 °C; 10% FBS with 0.1 mg/mL streptomycin and 100 U/mL penicillin in DMEM was then added for interruption of enzymatic activity. After centrifugation at 1500 rpm for 5 min, pellets were resuspended in DMEM with 10% FBS in a wet chamber at 37 °C/ 5% CO_2 until cell confluence. The cells were detached using 0.05% trypsin-EDTA solution. Cells were used at the fourth passage in all experiments [78].

2.4. Characterization of ADSCs

For surface marker analysis of the isolated ADSCs, cells were incubated with phycoerythrin-conjugated antibodies against murine CD29, CD44, CD90, CD45, CD31, and MHC II for 30 min at 4 °C. The cells were analyzed using a FACSAria III cytometer (Becton Dickinson, San Jose, CA) equipped with a 488 nm argon laser, and graphs were generated with WinMDI 9.2 software. The adipogenic and osteogenic differentiation of the MSCs was performed according to previously published protocols [66]. After 4% paraformaldehyde fixation, the calcium deposition and lipid droplets were stained with Alizarin Red S and Oil Red O solution, respectively.

2.5. Differentiation of mesenchymal stromal cells into insulin-producing cells (IPCs)

Cells used (in passage 4, P4) were cultured in triplicate in a 6-well plate (TPP) and had a confluence of > 80% (~4×10^5 cells/mL). Cells were incubated in a humidified atmosphere at 37 °C and 5% CO_2. Control cells were cultured with serum-free DMEM. To obtain IPCs (previously described by [78]), cells were maintained for 3 days in serum-free DMEM-F12 with 1% penicillin/streptomycin, supplemented with 10 nM nicotinamide (Sigma), 10 ng/mL activin-A (Sigma) and 10 nM exendin-4 (Sigma, St. Louis, MO).

2.6. Evaluation of glucose-stimulated insulin secretion

Insulin secretion into in the cell culture supernatant was measured by colorimetric assay (Labtest Diagnostica Kits), as indicated by the manufacturer, and employing the Labmax 240 equipment (Labtest Diagnóstica, Minas Gerais, Brazil). Briefly, the IPCs were incubated for 1 h, twice. Cells were washed carefully three times with DPBS and then incubated with DMEM without glucose and DMEM F12 (17.5 mM glucose), respectively. The two steps each lasted 1 h and cell supernatants were collected at the end for evaluation of insulin secretion. Medium insulin was measured again, two weeks later, in the absence of the differentiation inductors to confirm the maintenance of insulin secretion potential.

2.7. DM1 model and surgical procedure for IPC implantation

The DM1 model was induced by intraperitoneal (IP) injection of streptozotocin (STZ) (60 mg/kg in citrate buffer, pH 4.5). Animals with a glycemia of > 250 mg/dL were considered diabetic. A schematic representation of the experimental protocol is shown in Fig. 2 A. WKY rats were used to analyze the stromal and immunomodulatory effects of ADSCs and the effectiveness of cell treatment, using ADSCs differentiated into IPCs for the prevention of cognitive damage by untreated diabetes. The groups (8 male WKY rats per group) were divided into: Group I (Sham group): Animals injected with vehicle via IP injection and submitted to all surgical steps except transplantation. Group II, Group III and Group IV: Rats injected once with STZ (60 mg/kg body weight) via IP injection. Group II (diabetic group - STZ): Animals submitted to all surgical steps except transplantation. Group III (SCR -IPCs): Animals received IPCs transplanted into the subcapsular renal space (4×10^6 cells/rat) at 1 week after DM1 induction. Group IV (SC-IPCs): Animals received IPCs transplanted into the subcutaneous space (4×10^6 cells/rat), at 1 week after DM1 induction. Briefly, on the day

of the surgery, all animals were anesthetized with ketamine/xylazine (75 and 10 mg/kg, respectively, i.p.).

Surgical procedure for Subcapsular renal implantation: After trichotomy of the left inferior dorsolateral region, the kidney was exposed through a 1.5 cm incision and, with the aid of straight thin forceps, 4×10^6 cells were implanted under the renal capsule. After suturing the two planes with 7.0 suture wire the animal was placed on a heating plate and monitored until it presented reactions to external stimuli.

Surgical procedure for subcutaneous implantation: A longitudinal incision (0.5 cm) was made in the dorsal of the rat, the skin was separated from the underlying muscle with forceps and 4×10^6 cells were implanted in this subcutaneous space.

Similarly, following the same procedure and at the same sites, IPCs from adipose-derived mesenchymal stromal cells of green fluorescent protein (GFP-tg Lewis) rats were transplanted into Lewis rats subjected to diabetes mellitus (induced by STZ) for tracking the cells.

2.8. Glycemia control

Weekly blood glucose measurements were performed with a blood glucose monitor (Accu-Chek Advantage II-Roche) on 20-μL blood samples, collected by pricking the distal portion of animals' tails with an insulin needle.

2.9. Peptide C release

Measurement of peptide C content was performed using commercial rat/mouse ELISAs (Millipore), according to the manufacturer's instructions.

2.10. AGE measurement

AGEs were measured in the serum by ELISA, as previously described by Ikeda et al. [29] with some modifications. Briefly, the wells of a microtiter plate were coated overnight with 0.1 μg protein in 0.1 mL of 50 mM carbonate bicarbonate buffer (pH 9.6). The wells were washed with washing buffer (PBS containing 0.05% Tween 20) and then incubated for 3 h with 2% albumin. Subsequently, wells were washed again and incubated with 100 μL of anti-AGE (6D12) for 1 h. After washing, wells were incubated with 100 μL peroxidase-conjugated secondary antibody for 1 h. The reactivity of peroxidase was determined by incubation with OPD for 30 min. The reaction was stopped by the addition of 50 μL sulfuric acid (3 M). Absorbance measurements were taken at 492 nm. Results were calculated and expressed as a percentage of the control.

2.11. Novel recognition test (NOR)

The novel recognition test (NOR) is a task comprised of three phases; habituation, training and test performed in an open field apparatus (50 cm side). To habituate the animals, rats were placed in the lateral of the apparatus and allowed to freely explore the open-field arena in the absence of objects during 10 min. Twenty-four hours after the habituation phase, the animals underwent a training phase, where the rat was returned to the apparatus, which contained two identical sample objects (A + A). One hour and 24 h after the training phase, the rats were returned to the apparatus to test short-term (STM) or long-term (LTM) memory, respectively. In the test session, the rat was returned to the open-field arena, which contained two objects; one object was identical to that of the training session and the other object was novel (A + B). For LTM, the object 'B' was replaced by a third one 'C', and the 'A' object was maintained the same. The recognition index in each session was calculated as follows: time exploring the novel object/time exploring both objects. Exploration was defined as sniffing or touching the object with the nose and/or forepaws. The apparatus and the objects were thoroughly cleaned with 70% ethanol between the trials to ensure the absence of olfactory cues [7].

2.12. ELISA for S100B and GFAP

Hippocampal S100B content was measured by ELISA [42]. Briefly, 50 μL of sample plus 50 μL of Tris buffer were incubated for 2 h on a microtiter plate previously coated with monoclonal anti-S100B (SH-B1). Polyclonal anti-S100B was incubated for 30 min and then peroxidase-conjugated anti-rabbit antibody was added for a further 30 min. A colorimetric reaction with *o*-phenylenediamine was measured at 492 nm. The standard S100B curve ranged from 0.020 to 10 ng/mL. The ELISA for hippocampal GFAP [73] was carried out by coating the microtiter plate with 100 μL samples containing 30 μg of protein for 24 h at 4 °C. Incubation with a rabbit polyclonal anti-GFAP for 2 h was followed by incubation with a secondary antibody conjugated with peroxidase for 1 h, at room temperature; the standard GFAP curve ranged from 0.1 to 10 ng/mL.

2.13. Western blot analysis for synaptophysin

Proteins in the samples were homogenized in sample buffer (62.5 mM Tris–HCl, pH 6.8, 10% (*v*/v) glycerol, 2% (*w/v*) SDS, 5% (w/v) β-mercaptoethanol and 0.002% bromphenol blue) and separated by SDS-PAGE on 12% (w/v) acrylamide gel before electro transferring onto nitrocellulose membranes. The membranes were blocked with 2% chicken egg in tris-buffered saline with Tween 20 (TTBS) (20 mmol/L Tris–HCl, pH 7.5, 137 mmol/L NaCl, 0.05% (*v*/v) Tween 20) and then incubated overnight (4 °C). Subsequently, the membranes were incubated overnight with the appropriate primary antibodies: anti-synaptophysin (diluted 1:5000 in TTBS and 1% bovine standard albumin; BSA). Next, the membranes were incubated for 1 h at room temperature with secondary antibody, horseradish peroxidase (HRP)-conjugated anti-mouse IgG (1:10,000, Dako). Actin (Millipore; Darmstadt, Germany) was used as a loading control. Chemiluminescent bands were detected using Image Quant LAS4000 GE Healthcare, and densitometric analyses were performed using Image-J software. Results are expressed as percentages of the control.

2.14. Immunofluorescence

Rats were anesthetized using ketamine/xylazine and were perfused through the left cardiac ventricle with 200 mL of saline solution, followed by 200 mL of 4% paraformaldehyde in 0.1 M phosphate buffer, pH 7.4. The tissues were removed and left for post-fixation in the same fixative solution at 4 °C for 24 h. Subsequently, the material was cryoprotected by immersing the brain in 30% and 15% sucrose in phosphate buffer at 4 °C. The tissues were sectioned (40 μm) on a cryostat (Leitz) and the slices were put on the sheets. Sections were surrounded by a liquid blocker pen to help maintain the antibody solutions in contact with the slices. The slices were covered with Fluor save® and the images were captured using an Olympus confocal microscope [58].

2.15. Protein determination

Protein content was measured by Lowry's method with some modifications, using bovine serum albumin as the standard [55].

2.16. Statistical analysis

For blood glucose over time, parametric data from the experiments are presented as mean ± standard error and statistically evaluated by two-way analysis of variance, followed by the Tukey's test. Statistical comparisons between different groups were tested by one-way ANOVA followed by the Tukey's test. For the NOR test, data are presented as means ± S.E.M. and statistically evaluated by Student's *t*-test. For the

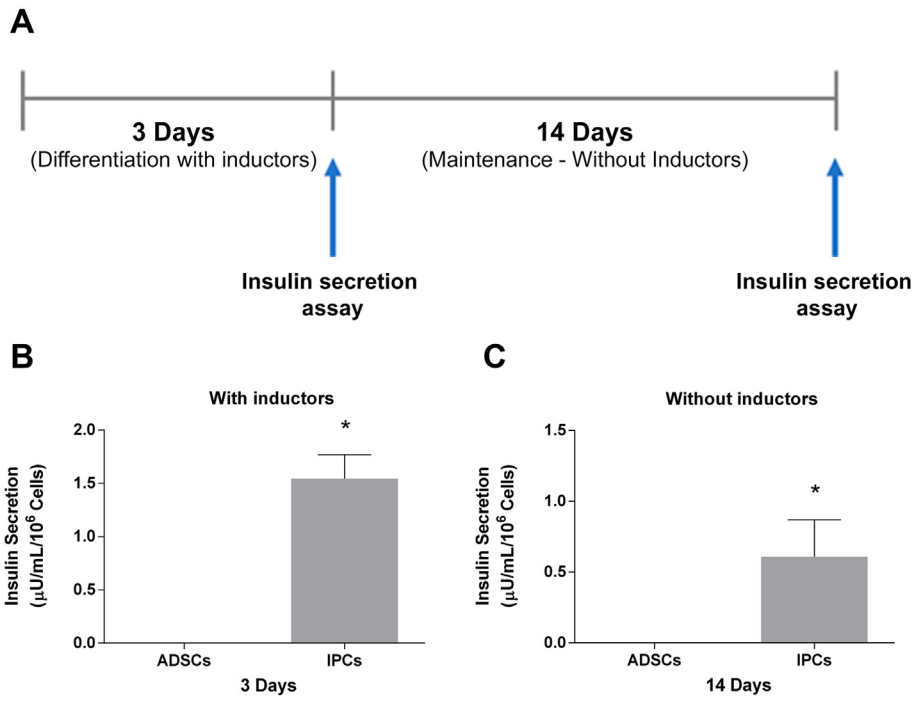

Fig. 1. In vitro *glucose-stimulated secretion of insulin in IPCs generated from ADSCs.* ADSCs were submitted to a short-term (3 days) differentiation protocol with inductors (nicotinamide/exendin-4/activin-A) to obtain insulin-producing cells (IPCs). A shows the timeline of the experiment. Glucose-stimulated secretion of insulin was evaluated immediately after differentiation (in B) and 14 days afterwards (in C), during this period they were maintained in culture, but in the absence of inductors. The insulin secretion, measured by colorimetric assay at 1 h after medium replacement, corresponds to the difference between the extracellular content of insulin in the presence (17.5 mM) and absence of glucose. Insulin secretion was significant (* Student *t*-test and $p < 0.05$), when compared with ADSCs at both times. Data are expressed as means ± SE of 6 independent experiments performed in triplicate.

evaluation of glucose-stimulated insulin secretion, statistical comparisons between different groups were made using repeated measures ANOVA followed by Tukey's test. Values of $P < 0.05$ were considered significant. All analyses were performed using the Graphpad Prism software version 6 (La Jolla, CA, USA).

3. Results

3.1. In vitro glucose-stimulated secretion of insulin in IPCs generated from ADSCs

ADSCs were submitted to a short-term (3 days) differentiation protocol to obtain insulin-producing cells (IPCs) containing nicotinamide/exendin-4/activing-A (inductors). Glucose-stimulated secretion of insulin was evaluated immediately after differentiation and 14 days afterwards; during this period they were maintained in culture, but in the absence of inductors. The experimental scheme is shown in Fig. 1A. Insulin secretion is compared with ADSCs cultured for the same time. Glucose-stimulated insulin secretion was performed by replacing the basal culture medium with medium containing 0 or 17.5 mM glucose. Insulin secretion, measured by colorimetric assay, at 1 h after medium replacement corresponds to the difference between the extracellular content of insulin in the presence and absence of glucose. Insulin secretion was clearly characterized, when compared with ADSCs (Fig. 1B, $p < 0.0001$). IPCs were able to secrete insulin after 2 weeks when stimulated by glucose, even when cultured in the absence of inductors (Fig. 1C, $p = 0.0323$).

3.2. Alterations in blood glucose, insulin and AGEs in diabetic rats are dependent on the via of IPC implantation

The diabetes mellitus model was induced by STZ and animals were included in the diabetic group when they exhibited a blood glucose of higher than 250 mg/dL (80% of animals). At one week after diabetes induction, rats were implanted with IPCs, which were administered by two different routes: subcapsular renal (SR) and subcutaneous (SC). The experimental schedule is shown in Fig. 2A.

Blood glucose was measured at one day, one week and two weeks after implantation to evaluate the effectiveness of IPCs for controlling glycemia (Fig. 2B, $p < 0.0001$ and $f_{(3,112)} = 116.0$). An increase in blood glucose was observed on the second day after STZ administration and in the following weeks in the STZ group. At one week after IPC implantation, blood glucose was reduced independently of the via of administration, although animals still presented high blood glucose levels compared to sham animals. Furthermore, STZ-treated animals demonstrated reduced body weight and this parameter was not altered by IPC implantation (data not shown).

Additionally, to confirm in vivo insulin secretion, we evaluated serum C-peptide in all experimental groups at two weeks after the implants (Fig. 2C, $p < 0.0001$ and $f_{(3.20)} = 5.938$). Elevated levels of C-peptide were observed in STZ rats that received IPCs by the SR route, while those that received the SC implant presented non-detectable peptide C levels. In order to evaluate long-term glucose toxicity, we determined serum AGE content and found an increase in AGE levels in diabetic rats, as expected. However, the implantation of IPCs at both implant sites (SR and SC) reversed this condition, returning levels to those found in sham group (Fig. 2D, $p = 0.0015$ and $f_{(3.20)} = 7.484$).

3.3. SC-implanted IPCs prevent cognitive impairment in diabetic rats

At three weeks after STZ-induced diabetes induction (or two weeks after the IPC implant), rats were submitted to cognitive evaluation, using the novel object recognition (NOR) test performed at 1 and 24 h to evaluate cognitive performance (short- and long-term memory, respectively). Results demonstrated that cognitive impairment was observed by three weeks after STZ exposure, when compared to the sham group, at both times evaluated. However, SR implantion of IPCs at one week after STZ was unable to prevent the cognitive deficit observed in diabetic rats, as evaluated by the NOR task at 1 h (Fig. 3A, p sham = 0.0149; p STZ = 0.4209; p SR = 0.2348) and at 24 h (p sham = 0.0020; p STZ = 0.5114; p SR = 0.3120). In contrast, interestingly, the SC implantation of IPCs was able to prevent the cognitive deficit found in diabetic rats, as evaluated by the NOR test at 1 h (Fig. 3C, p sham = 0.0005; p STZ = 0.3709; p SC = 0.0049) and at 24 h (p sham = 0.0012; p STZ = 0.0838; p SC = 0.0207).

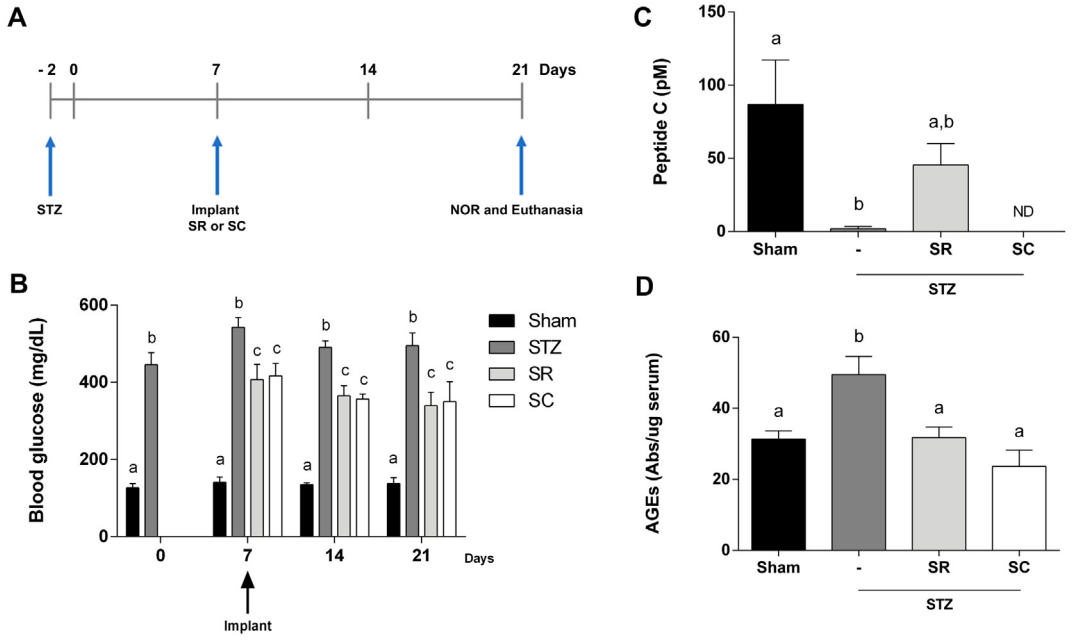

Fig. 2. *Effect of IPC implantation on blood glucose, insulin and AGEs in diabetic rats depends on the* via *of administration.* IPCs were implanted into the subcapsular renal (SR) or subcutaneous (SC) space in STZ diabetic Kyoto-Wistar rats. In A, timeline of the in vivo experiment. In B, blood glucose measurements before (−1 week) and after (1 and 2 weeks) the IPC implant. Groups were compared each week, by ANOVA. In C, C-peptide serum content measured by ELISA in the third week after IPC implantation. In D, serum AGE content, measured by ELISA, in the third week after IPC implantation. Data are expressed as means ± SE (8 rats in each group). Letters indicate different statistical groups by ANOVA followed by Tukey's test, assuming $p < 0.05$.

3.4. Hippocampal S100B content was reduced in diabetic rats and prevented by IPC implantation

Synaptophysin (neuronal marker), GFAP and S100B (glial markers) were investigated in the hippocampus. Synaptophysin content was not altered at 3 weeks after STZ admiynistration or by IPC implantation in either site (Fig. 4A, $F_{(3.21)} = 0.7500$, $p = 0.5345$). However, changes in glial markers were observed following procedures. Hippocampal GFAP was not altered in rats with STZ-induced diabetes at 3 weeks, but IPC implantation decreased GFAP, independently of implant via (Fig. 4B, $F_{(3.27)} = 6.642$, $p = 0.009$). On the other hand, S100B content was decreased in diabetic rats, and IPC implantation at both sites prevented

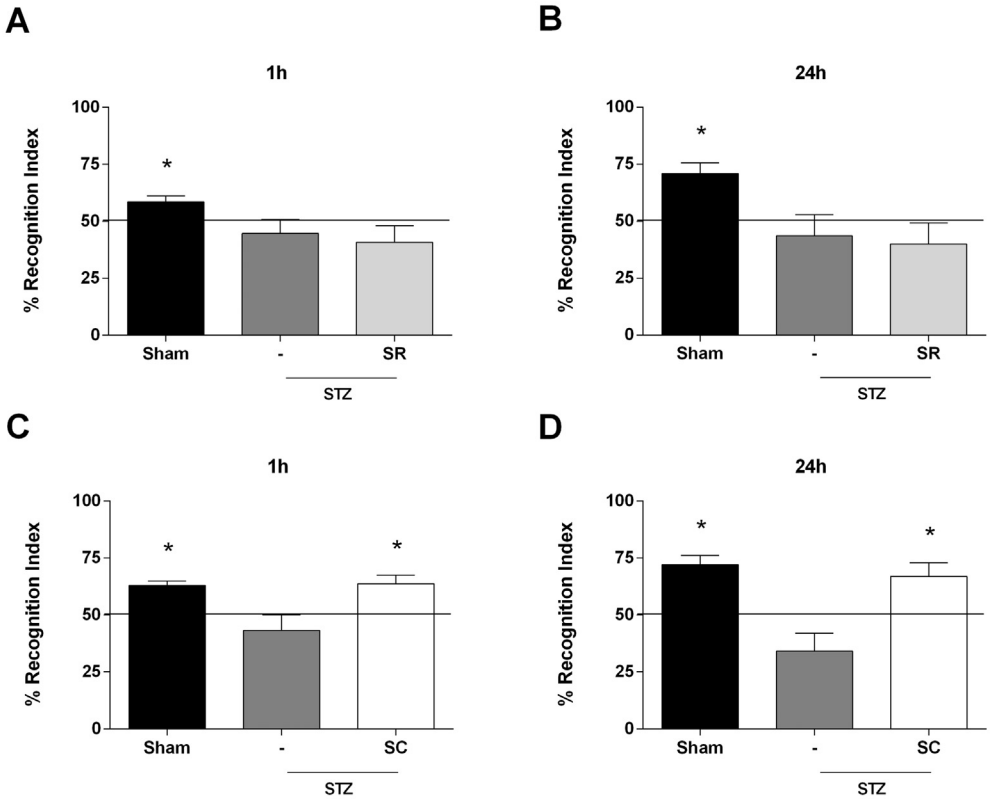

Fig. 3. Implantation of IPCs via SC, but not SR, prevented the cognitive impairment observed in diabetic rats. The cognitive performance of diabetic rats was determined at three weeks after STZ, using the NOR task at 1 h (for short-term memory) and 24 h (for long-term memory). IPC implantation was carried out in two different sites: subcapsular renal (SR) or subcutaneous (SC). In A, object recognition index of rats with or without SR implant of IPCs, 1 h after training trial. In B, object recognition index of rats with or without SR implant of IPCs, 24 h after training trial. In C, object recognition index of rats with or without SC implant of IPCs, 1 h after training trial. In D, object recognition index of rats with or without SC implant of IPCs, 24 h after training trial. * Statistically different from training trial (Student *t*-test, 8–9 rats/group, $p < 0.05$).

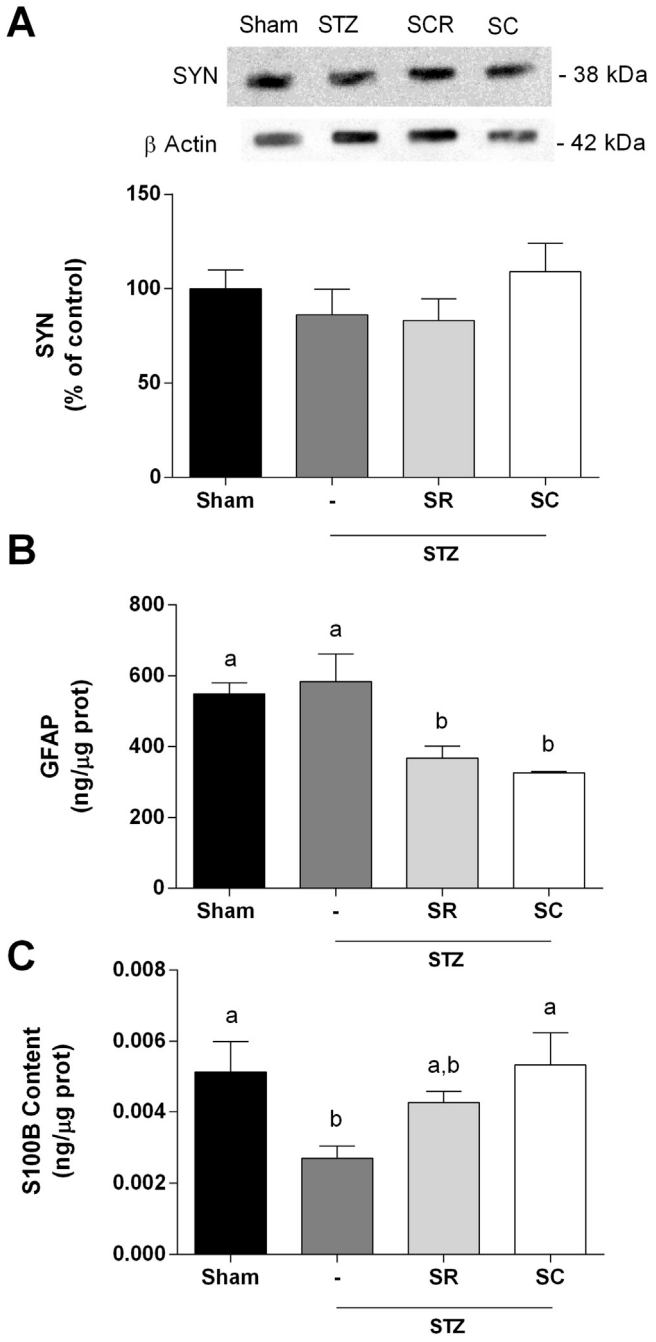

Fig. 4. *Cell markers in the hippocampus of diabetic rats after IPC implant.* Immunocontents of three cell markers were investigated in the hippocampus of diabetic rats at three weeks after STZ, in rats submitted or not to IPC implant (subcapsular renal, SR, or subcutaneous, SC). In A, the content of synaptophysin (SYN), measured by Western blotting. Representative blot containing bands of SYN and β-actin at the top of the panel. In B and C, the contents of GFAP and S100B, respectively, measured by ELISA. Data are expressed as means ± SE (8 rats/group). Letters indicate different statistical groups (ANOVA followed by Tukey's test, assuming $p < 0.05$).

this alteration; SR implantation partially inhibited the S100B decrease, while SC implantation completely abolished this decrease (Fig. 4C, $F_{(3.27)} = 3.937$, $p = 0.0188$).

3.5. IPCs survive and maintain undifferentiated morphology after implantation at both sites

Another set of experiments was performed using IPCs from GFP-labelled Lewis rats. GFP+ IPCs were implanted in SR or SC sites and rats were euthanized at 2 or 14 days after implantation. Histological analysis showed that the preparation of IPCs remained morphologically undifferentiated (i.e., they did not exhibit morphological characteristics of adipocytes or osteocytes) two days after the implantation in both sites. Panels A and B of Fig. 5 (magnified by 10 X and 40 X, respectively) show representative images at 2 days after IPC implantation in the SR site, and panels C and D show images at 2 days after implantation in the SC site (also magnified by 10 X and 40 X, respectively).

At fourteen days after implantation (Fig. 5 *E*-H), a decrease in GFP+ cell density in the graft was observed, as well as an apparent change in the cellular population at both implantation sites (SR and SC), as indicated by the presence of some differentiated adipocytes. Panels E and F of Fig. 5 show representative images at 14 days after implantation in the SR site (magnified by 10 X and 40 X, respectively) and panels G and H show images at 14 days after implantation in the SC site (also magnified by 10 X and 40 X, respectively).

3.6. GFP+ cells from IPC preparations migrate to the pancreas

We found GFP+ IPCs, implanted in both the SR and SC sites, in the STZ-damaged pancreas (Fig. 6). Within two days after implantation, there was a marked presence of GFP+ cells in pancreatic tissue, possibly attracted by signals of damaged tissue. However, when we compared both implant sites, the number of GPF+ cells in the pancreas of rats that received SC-implanted IPCs was more abundant than in the SR-implanted rats (Fig. 6, panels D and B, respectively). Over the course of two weeks, a greater fluorescence of GFP+ cells was still observed in the pancreatic tissue from SC-implanted rats than in pancreatic tissue from SR-implanted rats (Fig. 6, panels H and F, respectively). Interestingly, GFP + cells from the SC implant were organized in clusters in the pancreas than those placed in the SR 14 days after wards.

3.7. GFP+ cells from IPC preparations migrate to the hippocampus

Based on the cognitive improvement of diabetic rats, as evaluated by the NOR task, we investigated the presence of GFP^+ cells in the hippocampus, in the CA1 and DG regions (Fig. 7). At two days after SR (panels A and C, respectively) and SC (panels E and G, respectively) implantations, it was possible to observe GFP^+ cells around hippocampal vessels in the CA 1 and DG regions. However, at fourteen days after SC implantation, the number of GFP^+ cells increased in the CA1 (mainly) and DG regions (panels F and H, respectively). In contrast, in the SR-implanted rats, the number of GFP^+ cells in the CA1 and DG regions did not alter significantly from those observed at two days and remained around the blood vessels (panels B and D, respectively).

4. Discussion

Several strategies for DM treatment have been proposed over recent years. Insulin therapy achieves overall blood glucose control; however, glycemic variations occur during the intervals of administration, which could contribute to some of the complications of DM. Alternative therapies include the implantation of IPCs, which may be able to ameliorate hyperglycemia and even reverse DM. We have investigated approaches for the implantation of IPCs differentiated from ADSCs using a short-term protocol of culture with nicotinamide/exendin-4/activin A, as previously described by [78], emphasizing that they are not necessarily pancreatic beta cells, but cells capable to produce insulin and secrete it in response to glucose. In the present study, we compared the use of two different IPCs implantation sites (SR and SC) to investigate a putative protection against hippocampal damage induced by STZ in the DM1 rat model.

Our previous studies have demonstrated that IPCs can be obtained from ADSCs with a short-duration protocol, representing a chance to

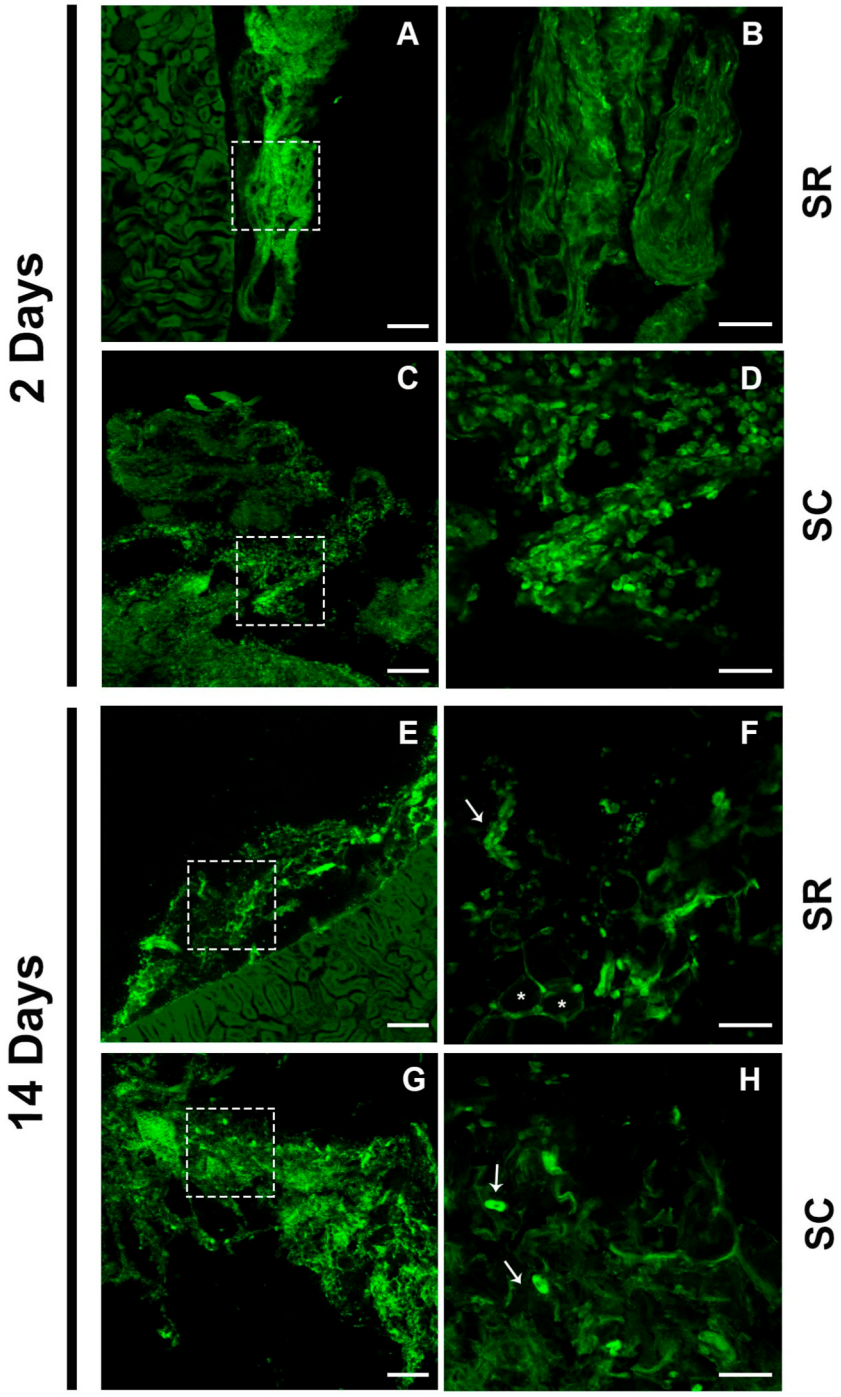

Fig. 5. *GFP+ cells of IPC preparations implanted at the subcapsular renal and subcutaneous implant sites.* IPCs were prepared from mesenchymal stromal cells of the adipose tissue of GFP-tg Lewis rats and implanted in the subcapsular renal (SR) or subcutaneous (SC) sites. In A and B, fluorescent images in the SR space, two days after implantation, magnified by 10× and 40× respectively. B corresponds to square in panel A. In C and D, fluorescent images in the SC space, at two days after implantation, magnified by 10× and 40× respectively. C corresponds to square in panel A. In E and F, fluorescent images in the SR space, at fourteen days after implantation, magnified by 10× and 40× by confocal microscopy, respectively. F corresponds to square in panel E. In G and H, fluorescent images in the SC space, at fourteen days after implantation, magnified by 10× and 40× respectively. H corresponds to square in panel G. Scale bars = 150 μm (left panels) and 50 μm (right panels). Arrows indicate nuclei of GFP+ cells and asterisks indicate adipocyte-like cells.

reduce costs and time in future investigations that employ these cells [78]. We confirmed that short-term differentiation (for 3 days) was enough to obtain active IPCs. Moreover, when IPCs were cultured for an additional 14 days, in the absence of inductors for IPC differentiation, they preserved their ability to secrete insulin. We chose this time because the diabetic animals were analyzed at 14 days after implantation.

The SR and SC sites were chosen for IPC implantation, based on advantages in terms of surgical feasibility, as well as the reported hyperglycemic control achieved [68,82]. Although many studies have investigated the ideal IPC implantation site for the reversal of hyperglycemia, none have compared the implantation sites with the aim of reducing the deleterious effects, caused by DM, on the CNS. Our results show that hyperglycemia was reduced after implantation at both sites, as observed in previous studies, including ours [71,78,80]. However, serum C-peptide was detected only in SR implanted rats, as also shown by other studies using IPCs for DM1 therapy [38,71,80].

Uncontrolled or prolonged hyperglycemia can lead to the formation of advanced glycation end products (AGEs), produced from non-enzymatic glycation and glycoxidation processes, and creating a pro-oxidant environment [76]. Glucotoxicity is one the causes of almost all complications of untreated DM, both peripherally and centrally [79]. Our results demonstrated that, as expected, diabetic rats presented an increase in serum AGE levels and, interestingly, after IPC implantation at both sites, serum AGEs returned to control levels. This effect may result from the presence of MSCs remaining, along with IPCs, in cell preparations, and these MSCs could provide an autophagic clearance behavior [28,44]. MSCs are capable of removing abnormal proteins or glycated amino acids, promoting cell repair in vivo [52]. Although the

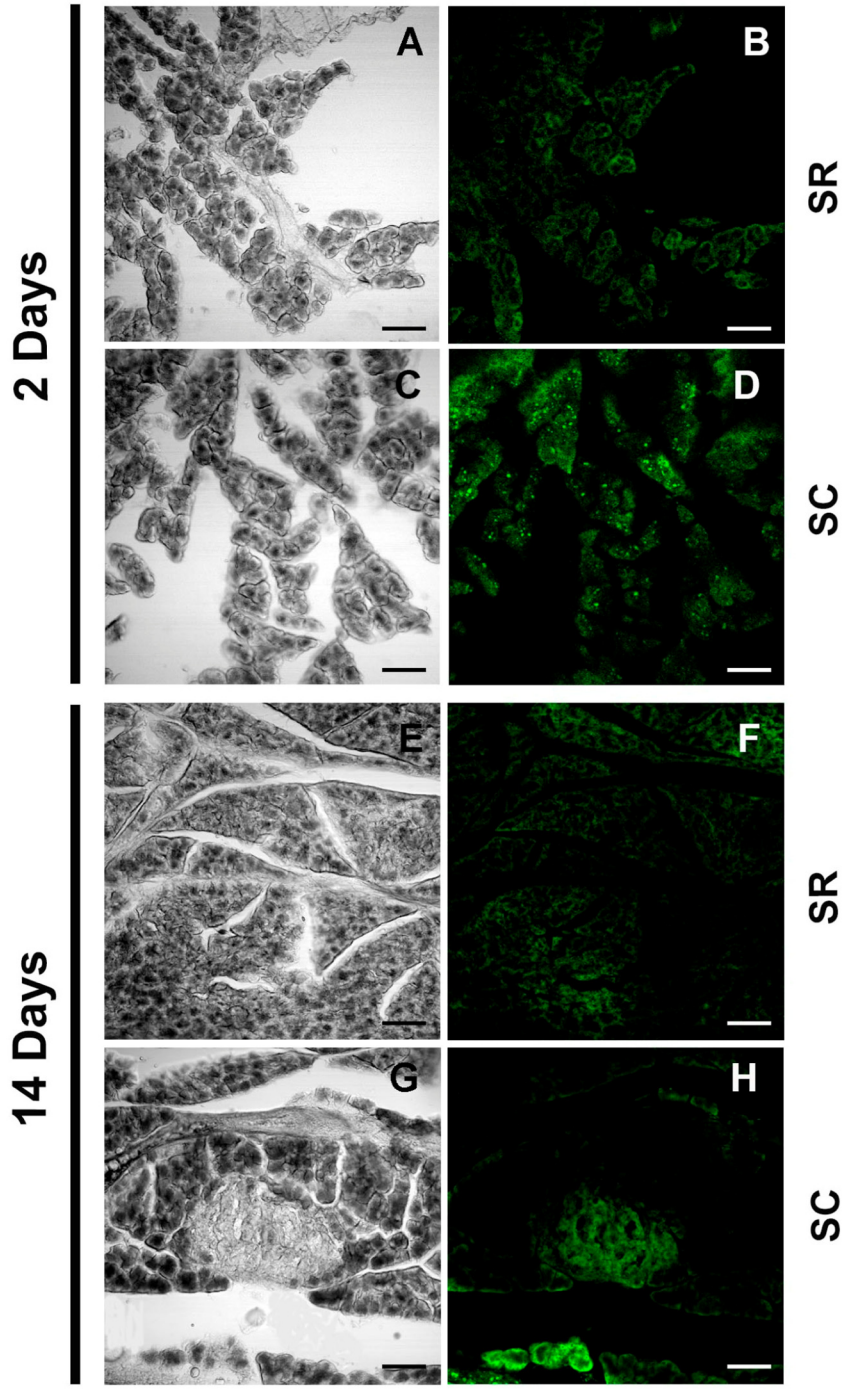

Fig. 6. *GFP+ cells of IPC preparations migrate to the pancreas of STZ-diabetic rats.* IPCs were prepared from mesenchymal stromal cells of the adipose tissue of GFP-tg Lewis rats and implanted in the subcapsular renal (SR) or subcutaneous (SC) sites. Corresponding phase contrast and fluorescent images, magnified 20×, from pancreatic tissue of transplanted diabetic rats are shown in the left and right panels, respectively. A and B, pancreatic tissue, two days after SR implant. C and D, two days after SC implant. E and F, fourteen days after SR implant. G and H, fourteen days after SC implant. Scale bar = 80 μm.

mechanisms of the autophagy activity and scavenging capacity of MSCs in DM1 are unclear, a scavenging capacity and AGE removal has been observed in diabetic wounds [25], removing intracellular β-amyloid [65], abnormal pulmonary epithelial cells [32,87] and alleviating beta cell damage [85].

Interestingly, based on the NOR task, the cognitive impairment observed in diabetic rats was prevented when IPCs were implanted via the SC space (but not via SR). SC-IPC implanted rats presented improvements in both short- and long-term memory. This cognitive improvement is not due to the hyperglycemia amelioration observed or due to the decrease in circulating AGEs, since these were detected in both the SR and SC groups. Based on the serum C-peptide content, it is also possible to rule out the cognitive improvement in the SC group due to increased insulin secretion.

Considering the fact that beneficial results in the CNS did not derive from changes in glycemia, AGEs and insulin, we consider a putative effect of the MSCs present in the cellular grafts. The benefits of the use of MSCs for the treatment of cognitive disorders has been well documented. Treatments with MSCs in animal models of Alzheimer's disease [15,86], as well as the effect of exosomes derived from MCSs [10,14],

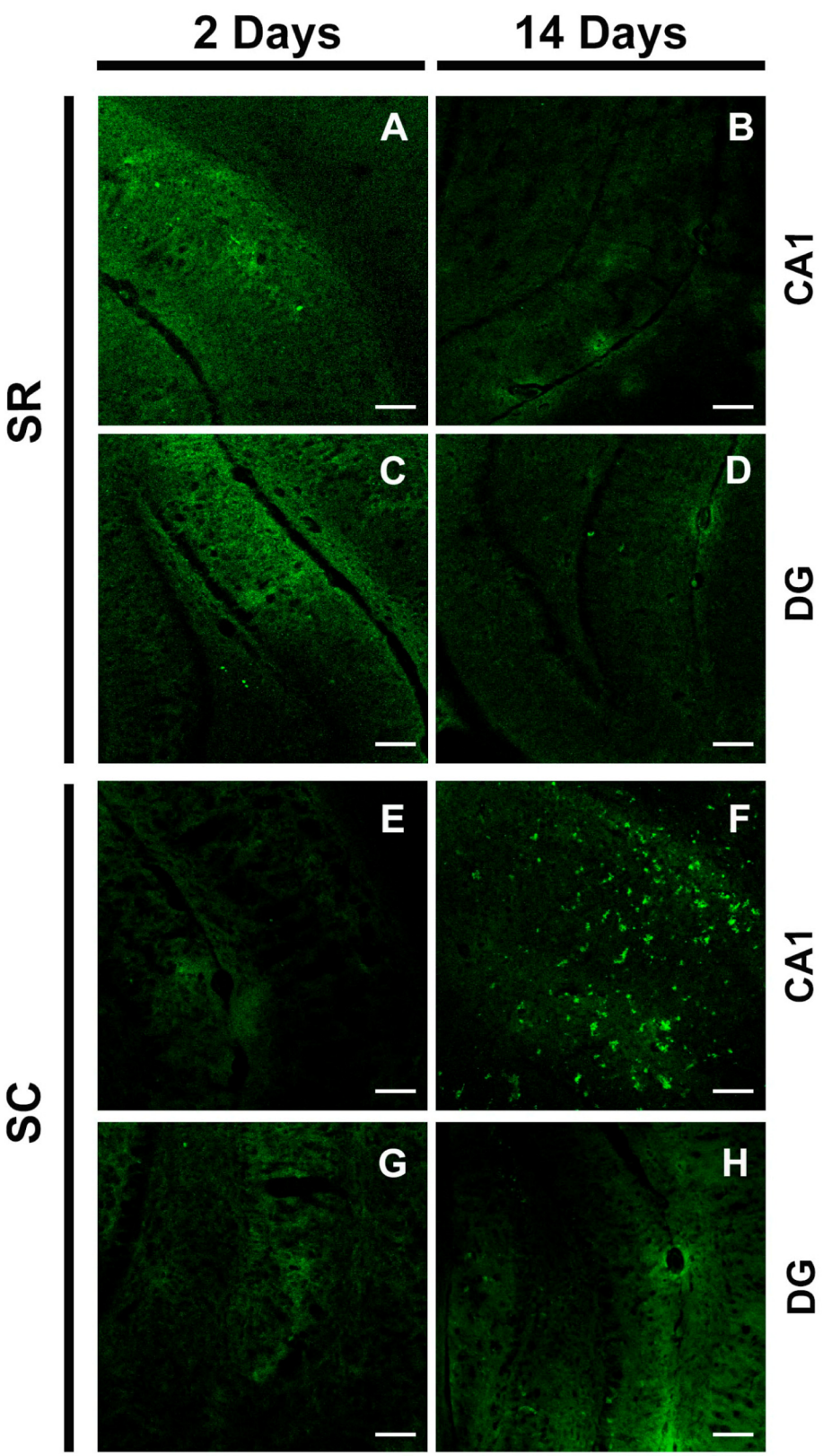

Fig. 7. *GFP+ cells of the IPC preparation migrate to the hippocampus of STZ-diabetic rats.* IPCs were prepared from mesenchymal stromal cells of the adipose tissue of GFP-tg Lewis rats and implanted in the subcapsular renal (SR) or subcutaneous (SC) sites. Presence of GFP+ cells was evaluated by confocal microscopy in CA1 and DG regions, magnified by 10×. A and B are images of the CA1 region, at two and fourteen days after SR implant, respectively. C and D are images of the DG region, at two and fourteen days after SR implant, respectively. E and F are images of the CA1 region, at two and fourteen days after SC implant, respectively. G and H are images of the DG region, at two and fourteen days after SC implant, respectively. Scale bar = 150 μm.

have been reported, as have their influence on cognitive deficits as a consequence of DM [48].

The MSCs have a homing capability, which allow the cells to navigate to regions of injury and inflammation, similarly to the response of leukocytes to cytokines [36,59], promoting tissue repair, including in the brain [74]. In fact, hippocampal damage can be signalled to different types of stem cells for migration and tissue repair in a series of injuries, such as traumatically injured brain [16], DA [43] and hippocampal ischemic/hypoxic injury [51]. Basically, systemic homing consists of a multistep process where cells from the circulation, or directly administered, reach a target site guided by chemical signals (see [50] for a review). It is well documented that none of the numerous

protocols available for obtaining IPCs result in complete cell differentiation (e.g. Gabr et al., 2014; [80]), even if in very small numbers, ADSCs are essential for the survival and functionality of the IPCs [21,53]. Therefore, our implant strategy (4×10^6 differentiated cells/rat) may not have provided enough IPCs for a reversal of the peripheral parameters of DM1; however, implantation in the SC region contributed to a total reversal of the cognition impairment observed. Assuming that IPCs lost their capacity for migration, the presence of MSCs could help explain cognitive improvements in diabetic rats. These cells could migrate to damaged brain sites in diabetic rats. However, it is unclear, at this time, as to why preparations of IPCs implanted in the SC site would provide more cells and/or more effective cells than cells implanted in the SR site, for improving hippocampal damage in diabetic rats.

We investigated two specific markers of astrocytes (GFAP and S100B), as well as synaptophysin, a neuron-specific marker, in the hippocampus of diabetic rats, submitted or not to IPC implantation. We did not find any alteration in hippocampal GFAP content at 3 weeks after STZ administration, but we observed a decrease in S100B in diabetic rats, in agreement with our previous report [49]. With regard to GFAP, conflicting results in the literature have reported increments, decrements and no changes in the hipocampal tissue [5,12,49,63]. It is also important to emphasize that, while GFAP is the most common marker of astrogliosis, its modulation does not indicate cellular dysfunction [2]. Herein, diabetic rats did not present changes in hippocampal GFAP, but when they received the IPC implant, independently of implantation in the SC or SC region, a decrease in GFAP was observed. Considering that GFAP expression increases with maturity and injury [81], we can postulate that astrocytes were “rejuvenated” by the presence of trophic factors released from implanted cells. This hypothesis requires further study involving other approaches.

With regard to hippocampal S100B, conflicting results exist, possibly due to methodological approaches. A transitory increase in S100B-positive cells has been reported at one week after STZ administration [41], which together with our current data, is in agreement with another study using a model of sporadic type Alzheimer's disease. Alzheimer's disease can offer a parallel for comparison, due to cognitive impairment and hippocampal astrocyte reactivity, and an increase in hippocampal S100B was described in the first week after induction, with a decrease later, in the fourth week [18]. S100B has many molecular targets in astrocytes, but is also secreted and has a trophic role in neurons via RAGE [17]. Interestingly, the decrease in S100B observed in diabetic animals was partially reversed by IPC implantation via SR and fully reversed via SC. This suggests a putative neurotrophic effect, mediated by S100B, in diabetic rats that received MSC/IPCs via SC.

Synaptophysin is a membrane protein of synaptic vesicles and related to neuronal plasticity of learning and memory, including in the NOR task [27]. We measured synaptophysin content and no changes were observed in hippocampal tissue, in agreement with another study performed in STZ-diabetic rats (also analyzed by Western blotting) [23]. We firstly hypothesized that a decrease in synaptophysin would occur in diabetic rats, but as seen for glial markers, there are conflicting results in the literature (e.g. [3,23]). However, we cannot exclude the possibility of specific local changes in this protein in the hippocampus, in association with the cognitive deficit observed in diabetic animals.

In another set of experiments, we used GFP+ cells to monitor the implant sites, at two and 14 days after the surgery, to determine whether cells survive at the implant site and if they migrate to potentially damaged sites, such as the pancreas and hippocampus. In this study, GFP+ cells from the preparation of IPCs were found in the pancreas, lungs and brain. We postulate that undifferentiated MSCs are present in our preparation, and these are able to migrate to remote sites [39,62].

Two days after IPC implantation, at both sites, we found clusters and isolated GFP+ cells. The cells at the SC site presented a looser arrangement than the cells at the SR site. This probably occurred because the kidney capsule is inelastic and has a limited space beneath it that cannot accommodate a large amount of cells, and that the cells were compressed under the kidney capsule [22]. With regard to remote organs, we observed cell migration from both implantation sites, but with different distribution profiles. Two days after implantation, GFP+ cells from the SC site were apparently more capable of migrating to the lungs (data not shown) and pancreas than to the hippocampal tissue. At this time, GFP+ cells in the hippocampus were found mainly around the blood vessels, consistent with the relative short period needed to complete migration and brain homing [33,50].

This scenario changed at two weeks after implantation. We still found a large number of GFP^+ cells at both SR and SC implant sites, but there was a reduction in the implanted cells that could be attributed to migration and cell death by local conditions (e.g. hypoxia) [20]. In fact, we observed the presence of adipocyte-like cells at both implant sites, which were apparently more numerous in the SR site than in the SC site. The presence of adipocytes was confirmed by oil red O staining (data not shown).

The SR site is commonly used for IPC implantation, where these cells remain producing insulin. In this study, GFP+ cells from the IPC preparation,n implanted at the SR and SC sites, were found in the pancreatic tissue. Interestingly, at 14 days after implantation in the SC site, GFP+ cells were more numerous and more organized in clusters in the pancreas than those placed in the SR. However, this greater “integration” with pancreatic tissue did not result in a recovery, considering the practically absent insulin secretion in SC implanted animals.

At 14 days, GFP+ cells implanted at the SC site were found in greater quantity and more scattered in the hippocampus than cells implanted at the SR site, particularly in the CA1 region of the hippocampus, as compared to the dentate gyrus region. In fact, GFP+ cells implanted at the SR site remained around the vessels for longer in both the hippocampal regions. In contrast to observations in the pancreas, the presence of GFP+ cells from the SC implant could be associated with the cognitive recovery observed in these animals.

MSCs and their products (exosomes, growth factors and cytokines) have been used to protect brain tissues against several types of injury, and their main action in brain repair may be due to the anti-inflammatory and immunosuppressive activities of these cells [54,56,64,74]. Accordingly, our data show a decrease in GFAP and S100B level recovery in the hippocampus of STZ-diabetic animals receiving IPCs, particularly at the SC site. Moreover, locally transplanted MSCs may stimulate hippocampal neurogenesis [24]. Cognitive impairment in STZ-diabetic rats has been reversed by treatment with MSCs administered intravenously and by intranasal administration of exosomes from these cells, suggesting that soluble MSCs are mediators of neuroprotection [48,60]. Although differences exist between bone marrow and adipose tissue MSCs, it is conceivable that the cognitive improvement observed in STZ-diabetic rats, in this study, is also due to the factors released by MSCs still present in our preparation of IPCs. Apparently, these MSCs survive, migrate and/or release trophic mediators when implanted at the SC site for reasons unclear at this moment. For example, it is possible that the richer blood supply at the SC site (increased after surgery) could explain, in part, the greater cell survival and migration [26,57].

5. Conclusions

In the present study, IPCs were implanted at two different sites (SC and SR) in STZ-diabetic rats. The cells implanted in the SC site successfully ameliorated cognitive impairment and modulated hippocampal parameters, such as S100B and GFAP. Peripherally, both implants improved hyperglycemia and caused a reduction in AGEs in diabetic rats, but serum insulin was not observed in the SC group. Using GFP+ cell implants, we observed the survival of these cells at the implant sites, as well as their migration to the pancreas and hippocampus. These data suggest the presence of undifferentiated MSCs in our IPC preparation, which could help to explain the peripheral reduction of

AGEs (by autophagic depuration) and the recovery of cognitive impairment (by immunomodulation at the hippocampus). Together, these data reinforce the importance of MSCs in neuroprotective strategies, and highlight the logistic importance of the subcutaneous route for administration.

Data availability

The data used to support the findings of this study are available from the corresponding author upon request.

Acknowledgments

This study was supported by the Conselho Nacional de Desenvolvimento Científico e Tecnológico (CNPq), Coordenação de Aperfeiçoamento de Pessoal de Nível Superior (CAPES), Fundação de Amparo à Pesquisa do Estado do Rio Grande do Sul (FAPERGS), Universidade Federal do Rio Grande do Sul, and Instituto Nacional de Ciência e Tecnologia para Excitotoxicidade e Neuroproteção (INCTEN/CNPq).

Contribution statement

P.S., C.A.G. and K.M.W. designed the study. K.M.W., L.R., L.J.L., B.C.F., N.G.S., A. M., and P.S. performed laboratory experiments and collected data. K.M.W. and P.S. performed statistical analyses. P.S., C.A.G., K.M.W. and L.R. wrote the manuscript. All authors edited and approved the manuscript.

Declaration of competing interest

The authors declare that they have no conflicts of interest.

References

[1] C. Aguayo-Mazzucato, S. Bonner-Weir, Pancreatic β cell regeneration as a possible therapy for diabetes, Cell Metab. 27 (2018) 57–67.
[2] M.A. Anderson, Y. Ao, M.V. Sofroniew, Heterogeneity of reactive astrocytes, Neurosci. Lett. 565 (2014) 23–29.
[3] F.I. Baptista, M.J. Pinto, F. Elvas, R.D. Almeida, A.F. Ambrósio, Diabetes alters KIF1A and KIF5B motor proteins in the hippocampus, PLoS One 8 (2013) e65515.
[4] B. Bauduceau, J. Doucet, L. Bordier, C. Garcia, O. Dupuy, H. Mayaudon, Hypoglycaemia and dementia in diabetic patients, Diabetes Metab. 36 (Suppl. 3) (2010) S106–S111.
[5] G. Baydas, V.S. Nedzvetskii, P.A. Nerush, S.V. Kirichenko, T. Yoldas, Altered expression of NCAM in hippocampus and cortex may underlie memory and learning deficits in rats with streptozotocin-induced diabetes mellitus, Life Sci. 73 (2003) 1907–1916.
[6] T.L. van Belle, K.T. Coppieters, M.G. von Herrath, Type 1 diabetes: etiology, immunology, and therapeutic strategies, Physiol. Rev. 91 (2011) 79–118.
[7] R. Biasibetti, J.P. Almeida Dos Santos, L. Rodrigues, K.M. Wartchow, L.Z. Suardi, P. Nardin, N.G. Selistre, D. Vázquez, C.-A. Gonçalves, Hippocampal changes in STZ-model of Alzheimer's disease are dependent on sex, Behav. Brain Res. 316 (2017) 205–214.
[8] A. Bruni, B. Gala-Lopez, A.R. Pepper, N.S. Abualhassan, A.J. Shapiro, Islet cell transplantation for the treatment of type 1 diabetes: recent advances and future challenges, Diabetes Metab. Syndr. Obes. Targets Ther. 7 (2014) 211–223.
[9] V. Chandra, G. Swetha, S. Muthyala, A.K. Jaiswal, J.R. Bellare, P.D. Nair, R.R. Bhonde, Islet-like cell aggregates generated from human adipose tissue derived stem cells ameliorate experimental diabetes in mice, PLoS One 6 (2011) e20615.
[10] S.-Y. Chen, M.-C. Lin, J.-S. Tsai, P.-L. He, W.-T. Luo, H. Herschman, H.-J. Li, EP4 antagonist-elicited extracellular vesicles from mesenchymal stem cells rescue cognition/learning deficiencies by restoring brain cellular functions, Stem Cells Transl. Med. 8 (2019) 707–723.
[11] P. Chhabra, K.L. Brayman, Stem cell therapy to cure type 1 diabetes: from hype to hope, Stem Cells Transl. Med. 2 (2013) 328–336.
[12] E.S. Coleman, J.C. Dennis, T.D. Braden, R.L. Judd, P. Posner, Insulin treatment prevents diabetes-induced alterations in astrocyte glutamate uptake and GFAP content in rats at 4 and 8 weeks of diabetes duration, Brain Res. 1306 (2010) 131–141.
[13] W.F. Coutinho, W.S. Silva Júnior, Diabetes Care in Brazil, Ann. Glob. Health 81 (2015) 735–741.
[14] G.-H. Cui, J. Wu, F.-F. Mou, W.-H. Xie, F.-B. Wang, Q.-L. Wang, J. Fang, Y.-W. Xu, Y.-R. Dong, J.-R. Liu, et al., Exosomes derived from hypoxia-preconditioned mesenchymal stromal cells ameliorate cognitive decline by rescuing synaptic dysfunction and regulating inflammatory responses in APP/PS1 mice, FASEB J. Off. Publ. Fed. Am. Soc. Exp. Biol. 32 (2018) 654–668.
[15] Y. Cui, S. Ma, C. Zhang, W. Cao, M. Liu, D. Li, P. Lv, Q. Xing, R. Qu, N. Yao, et al., Human umbilical cord mesenchymal stem cells transplantation improves cognitive function in Alzheimer's disease mice by decreasing oxidative stress and promoting hippocampal neurogenesis, Behav. Brain Res. 320 (2017) 291–301.
[16] J. Deng, Z. Zou, T. Zhou, Y. Su, G. Ai, J. Wang, H. Xu, S. Dong, Bone marrow mesenchymal stem cells can be mobilized into peripheral blood by G-CSF in vivo and integrate into traumatically injured cerebral tissue, Neurol. Sci. Off. J. Ital. Neurol. Soc. Ital. Soc. Clin. Neurophysiol. 32 (2011) 641–651.
[17] R. Donato, G. Sorci, F. Riuzzi, C. Arcuri, R. Bianchi, F. Brozzi, C. Tubaro, I. Giambanco, S100B's double life: intracellular regulator and extracellular signal, Biochim. Biophys. Acta 1793 (2009) 1008–1022.
[18] J.P.A. Dos Santos, A. Vizuete, F. Hansen, R. Biasibetti, C.-A. Gonçalves, Early and persistent O-GlcNAc protein modification in the Streptozotocin model of Alzheimer's disease, J. Alzheimers Dis. JAD 61 (2018) 237–249.
[19] Drive, A.D.A. 2451 C., Arlington, S. 900, and Va 22202 1–800-Diabetes Statistics about Diabetes.
[20] G. Faleo, H.A. Russ, S. Wisel, A.V. Parent, V. Nguyen, G.G. Nair, J.E. Freise, K.E. Villanueva, G.L. Szot, M. Hebrok, et al., Mitigating ischemic injury of stem cell-derived insulin-producing cells after transplant, Stem Cell Rep 9 (2017) 807–819.
[21] M. Figliuzzi, R. Cornolti, N. Perico, C. Rota, M. Morigi, G. Remuzzi, A. Remuzzi, A. Benigni, Bone marrow-derived mesenchymal stem cells improve islet graft function in diabetic rats, Transplant. Proc. 41 (2009) 1797–1800.
[22] D.W. Gray, R. Sutton, P. McShane, M. Peters, P.J. Morris, Exocrine contamination impairs implantation of pancreatic islets transplanted beneath the kidney capsule, J. Surg. Res. 45 (1988) 432–442.
[23] C.A. Grillo, G.G. Piroli, G.E. Wood, L.R. Reznikov, B.S. McEwen, L.P. Reagan, Immunocytochemical analysis of synaptic proteins provides new insights into diabetes-mediated plasticity in the rat hippocampus, Neuroscience 136 (2005) 477–486.
[24] K.N. Hamisha, M. Tfilin, J. Yanai, G. Turgeman, Mesenchymal stem cells can prevent alterations in behavior and neurogenesis induced by Aß25-35 administration, J. Mol. Neurosci. MN 55 (2015) 1006–1013.
[25] Y. Han, T. Sun, R. Tao, Y. Han, J. Liu, Clinical application prospect of umbilical cord-derived mesenchymal stem cells on clearance of advanced glycation end products through autophagy on diabetic wound, Eur. J. Med. Res. 22 (2017) 11.
[26] Y. Hayashi, M. Murakami, R. Kawamura, R. Ishizaka, O. Fukuta, M. Nakashima, CXCL14 and MCP1 are potent trophic factors associated with cell migration and angiogenesis leading to higher regenerative potential of dental pulp side population cells, Stem Cell Res Ther 6 (2015) 111.
[27] E.M. Hernández-Hernández, K. Caporal Hernandez, R.A. Vázquez-Roque, A. Díaz, F. de la Cruz, B. Florán, G. Flores, The neuropeptide-12 improves recognition memory and neuronal plasticity of the limbic system in old rats, Synap. N. Y. N 72 (2018) e22036.
[28] C. Hu, L. Zhao, D. Wu, L. Li, Modulating autophagy in mesenchymal stem cells effectively protects against hypoxia- or ischemia-induced injury, Stem Cell Res Ther 10 (2019) 120.
[29] K. Ikeda, T. Higashi, H. Sano, Y. Jinnouchi, M. Yoshida, T. Araki, S. Ueda, S. Horiuchi, N (epsilon)-(carboxymethyl)lysine protein adduct is a major immunological epitope in proteins modified with advanced glycation end products of the Maillard reaction, Biochemistry 35 (1996) 8075–8083.
[30] L. Jing, L. Mai, J.-Z. Zhang, J.-G. Wang, Y. Chang, J.-D. Dong, F.-Y. Guo, P.A. Li, Diabetes inhibits cerebral ischemia-induced astrocyte activation - an observation in the cingulate cortex, Int. J. Biol. Sci. 9 (2013) 980–988.
[31] C.G. Jolivalt, R. Hurford, C.A. Lee, W. Dumaop, E. Rockenstein, E. Masliah, Type 1 diabetes exaggerates features of Alzheimer's disease in APP transgenic mice, Exp. Neurol. 223 (2010) 422–431.
[32] J. Jung, J.H. Choi, Y. Lee, J.-W. Park, I.-H. Oh, S.-G. Hwang, K.-S. Kim, G.J. Kim, Human placenta-derived mesenchymal stem cells promote hepatic regeneration in CCl4 -injured rat liver model via increased autophagic mechanism, Stem Cells Dayt. Ohio 31 (2013) 1584–1596.
[33] S. Kalimuthu, J.M. Oh, P. Gangadaran, L. Zhu, H.W. Lee, R.L. Rajendran, S.H. Baek, Y.H. Jeon, S.Y. Jeong, S.-W. Lee, et al., In vivo tracking of chemokine receptor CXCR4-engineered Mesenchymal stem cell migration by optical molecular imaging, Stem Cells Int. 2017 (2017) 8085637.
[34] O. Karnieli, Y. Izhar-Prato, S. Bulvik, S. Efrat, Generation of insulin-producing cells from human bone marrow mesenchymal stem cells by genetic manipulation, Stem Cells Dayt. Ohio 25 (2007) 2837–2844.
[35] S. Kern, H. Eichler, J. Stoeve, H. Klüter, K. Bieback, Comparative analysis of mesenchymal stem cells from bone marrow, umbilical cord blood, or adipose tissue, Stem Cells Dayt. Ohio 24 (2006) 1294–1301.
[36] S. Kidd, E. Spaeth, J.L. Dembinski, M. Dietrich, K. Watson, A. Klopp, V.L. Battula, M. Weil, M. Andreeff, F.C. Marini, Direct evidence of mesenchymal stem cell tropism for tumor and wounding microenvironments using in vivo bioluminescent imaging, Stem Cells Dayt. Ohio 27 (2009) 2614–2623.
[37] B. Klimova, K. Kuca, P. Maresova, Global view on Alzheimer's disease and diabetes mellitus: threats, risks and treatment Alzheimer's disease and diabetes mellitus, Curr. Alzheimer Res. 15 (2018) 1277–1282.
[38] Y. Kondo, T. Toyoda, R. Ito, M. Funato, Y. Hosokawa, S. Matsui, T. Sudo, M. Nakamura, C. Okada, X. Zhuang, et al., Identification of a small molecule that facilitates the differentiation of human iPSCs/ESCs and mouse embryonic pancreatic explants into pancreatic endocrine cells, Diabetologia 60 (2017) 1454–1466.
[39] A. Kurtz, Mesenchymal stem cell delivery routes and fate, Int. J. Stem Cells 1 (2008) 1–7.
[40] P.E. Lacy, C. Ricordi, E.H. Finke, Effect of transplantation site and alpha L3T4

treatment on survival of rat, hamster, and rabbit islet xenografts in mice, Transplantation 47 (1989) 761–766.
[41] Y.V. Lebed, M.A. Orlovsky, A.G. Nikonenko, G.A. Ushakova, G.G. Skibo, Early reaction of astroglial cells in rat hippocampus to streptozotocin-induced diabetes, Neurosci. Lett. 444 (2008) 181–185.
[42] M.C. Leite, F. Galland, G. Brolese, M.C. Guerra, J.W. Bortolotto, R. Freitas, L.M.V. de Almeida, C. Gottfried, C.-A. Gonçalves, A simple, sensitive and widely applicable ELISA for S100B: methodological features of the measurement of this glial protein, J. Neurosci. Methods 169 (2008) 93–99.
[43] J.-S. Li, Z.-X. Yao, Modulation of FGF receptor signaling as an intervention and potential therapy for myelin breakdown in Alzheimer's disease, Med. Hypotheses 80 (2013) 341–344.
[44] W. Li, K. Li, J. Gao, Z. Yang, Autophagy is required for human umbilical cord mesenchymal stem cells to improve spatial working memory in APP/PS1 transgenic mouse model, Stem Cell Res Ther 9 (2018).
[45] Y.-C. Lin, H.-J. Harn, P.-C. Lin, M.-H. Chuang, C.-H. Chen, S.-Z. Lin, T.-W. Chiou, Commercial production of autologous stem cells and their therapeutic potential for liver cirrhosis, Cell Transplant. 26 (2017) 449–460.
[46] X.-Y. Mao, D.-F. Cao, X. Li, J.-Y. Yin, Z.-B. Wang, Y. Zhang, C.-X. Mao, H.-H. Zhou, Z.-Q. Liu, Huperzine a ameliorates cognitive deficits in streptozotocin-induced diabetic rats, Int. J. Mol. Sci. 15 (2014) 7667–7683.
[47] A. Mellgren, A.H. Schnell Landström, B. Petersson, A. Andersson, The renal subcapsular site offers better growth conditions for transplanted mouse pancreatic islet cells than the liver or spleen, Diabetologia 29 (1986) 670–672.
[48] M. Nakano, K. Nagaishi, N. Konari, Y. Saito, T. Chikenji, Y. Mizue, M. Fujimiya, Bone marrow-derived mesenchymal stem cells improve diabetes-induced cognitive impairment by exosome transfer into damaged neurons and astrocytes, Sci. Rep. 6 (2016) 24805.
[49] P. Nardin, C. Zanotto, F. Hansen, C. Batassini, M.S. Gasparin, P. Sesterheim, C.-A. Gonçalves, Peripheral levels of AGEs and astrocyte alterations in the hippocampus of STZ-diabetic rats, Neurochem. Res. 41 (2016) 2006–2016.
[50] F. Nitzsche, C. Müller, B. Lukomska, J. Jolkkonen, A. Deten, J. Boltze, Concise review: MSC adhesion Cascade-insights into homing and Transendothelial migration, Stem Cells Dayt. Ohio 35 (2017) 1446–1460.
[51] E. Nivet, M. Vignes, S.D. Girard, C. Pierrisnard, N. Baril, A. Devèze, J. Magnan, F. Lanté, M. Khrestchatisky, F. Féron, et al., Engraftment of human nasal olfactory stem cells restores neuroplasticity in mice with hippocampal lesions, J. Clin. Invest. 121 (2011) 2808–2820.
[52] H.J. Park, J.Y. Shin, H.N. Kim, S.H. Oh, P.H. Lee, Neuroprotective effects of mesenchymal stem cells through autophagy modulation in a parkinsonian model, Neurobiol. Aging 35 (2014) 1920–1928.
[53] K.S. Park, Y.S. Kim, J.H. Kim, B.K. Choi, S.H. Kim, S.H. Oh, Y.R. Ahn, M.S. Lee, M.K. Lee, J.B. Park, et al., Influence of human allogenic bone marrow and cord blood-derived mesenchymal stem cell secreting trophic factors on ATP (adenosine-5′-triphosphate)/ADP (adenosine-5′-diphosphate) ratio and insulin secretory function of isolated human islets from cadaveric donor, Transplant. Proc. 41 (2009) 3813–3818.
[54] G. Paul, S.V. Anisimov, The secretome of mesenchymal stem cells: potential implications for neuroregeneration, Biochimie 95 (2013) 2246–2256.
[55] G.L. Peterson, A simplification of the protein assay method of Lowry et al. which is more generally applicable, Anal. Biochem. 83 (1977) 346–356.
[56] C.L. Rackham, S. Amisten, S.J. Persaud, A.J.F. King, P.M. Jones, Mesenchymal stromal cell secretory factors induce sustained improvements in islet function pre- and post-transplantation, Cytotherapy 20 (2018) 1427–1436.
[57] A. Rajab, Islet transplantation: alternative sites, Curr. Diab. Rep. 10 (2010) 332–337.
[58] L. Rodrigues, K.M. Wartchow, L.Z. Suardi, B.C. Federhen, N.G. Selistre, C.-A. Gonçalves, Streptozotocin causes acute responses on hippocampal S100B and BDNF proteins linked to glucose metabolism alterations, Neurochem. Int. 128 (2019) 85–93.
[59] B. Rüster, S. Göttig, R.J. Ludwig, R. Bistrian, S. Müller, E. Seifried, J. Gille, R. Henschler, Mesenchymal stem cells display coordinated rolling and adhesion behavior on endothelial cells, Blood 108 (2006) 3938–3944.
[60] J. Ruzicka, M. Kulijewicz-Nawrot, J.J. Rodrigez-Arellano, P. Jendelova, E. Sykova, Mesenchymal stem cells preserve working memory in the 3xTg-AD mouse model of Alzheimer's disease, Int. J. Mol. Sci. 17 (2016).
[61] T. Sapir, K. Shternhall, I. Meivar-Levy, T. Blumenfeld, H. Cohen, E. Skutelsky, S. Eventov-Friedman, I. Barshack, I. Goldberg, S. Pri-Chen, et al., Cell-replacement therapy for diabetes: generating functional insulin-producing tissue from adult human liver cells, Proc. Natl. Acad. Sci. U. S. A. 102 (2005) 7964–7969.
[62] A. Schmidt, D. Ladage, C. Steingen, K. Brixius, T. Schinköthe, F.-J. Klinz, R.H.G. Schwinger, U. Mehlhorn, W. Bloch, Mesenchymal stem cells transmigrate over the endothelial barrier, Eur. J. Cell Biol. 85 (2006) 1179–1188.
[63] P.N. de Senna, J. Ilha, P.P.A. Baptista, P.S. do Nascimento, M.C. Leite, M.F. Paim, C.A. Gonçalves, M. Achaval, L.L. Xavier, Effects of physical exercise on spatial memory and astroglial alterations in the hippocampus of diabetic rats, Metab. Brain Dis. 26 (2011) 269–279.
[64] L.S. Sherman, M.P. Romagano, S.F. Williams, P. Rameshwar, Mesenchymal stem cell therapies in brain disease, Semin. Cell Dev. Biol. 95 (2019) 111–119.
[65] J.Y. Shin, H.J. Park, H.N. Kim, S.H. Oh, J.-S. Bae, H.-J. Ha, P.H. Lee, Mesenchymal stem cells enhance autophagy and increase β-amyloid clearance in Alzheimer disease models, Autophagy 10 (2014) 32–44.
[66] L. da Silva Meirelles, P.C. Chagastelles, N.B. Nardi, Mesenchymal stem cells reside in virtually all post-natal organs and tissues, J. Cell Sci. 119 (2006) 2204–2213.
[67] J.S. Skyler, Hope vs hype: where are we in type 1 diabetes? Diabetologia 61 (2018) 509–516.
[68] R.A. Stokes, K. Cheng, A. Lalwani, M.M. Swarbrick, H.E. Thomas, T. Loudovaris, T.W. Kay, W.J. Hawthorne, P.J. O'Connell, J.E. Gunton, Transplantation sites for human and murine islets, Diabetologia 60 (2017) 1961–1971.
[69] Y. Sun, L. Chen, X. Hou, W. Hou, J. Dong, L. Sun, K. Tang, B. Wang, J. Song, H. Li, et al., Differentiation of bone marrow-derived mesenchymal stem cells from diabetic patients into insulin-producing cells in vitro, Chin. Med. J. 120 (2007) 771–776.
[70] G.L. Szot, P. Koudria, J.A. Bluestone, Transplantation of pancreatic islets into the kidney capsule of diabetic mice, J. Vis. Exp. JoVE 404 (2007).
[71] D. Talavera-Adame, O.O. Woolcott, J. Ignatius-Irudayam, V. Arumugaswami, D.H. Geller, D.C. Dafoe, Effective endothelial cell and human pluripotent stem cell interactions generate functional insulin-producing beta cells, Diabetologia 59 (2016) 2378–2386.
[72] K. Timper, D. Seboek, M. Eberhardt, P. Linscheid, M. Christ-Crain, U. Keller, B. Müller, H. Zulewski, Human adipose tissue-derived mesenchymal stem cells differentiate into insulin, somatostatin, and glucagon expressing cells, Biochem. Biophys. Res. Commun. 341 (2006) 1135–1140.
[73] F. Tramontina, M.C. Leite, K. Cereser, D.F. de Souza, A.C. Tramontina, P. Nardin, A.C. Andreazza, C. Gottfried, F. Kapczinski, C.-A. Gonçalves, Immunoassay for glial fibrillary acidic protein: antigen recognition is affected by its phosphorylation state, J. Neurosci. Methods 162 (2007) 282–286.
[74] D. Ulrich, S.L. Edwards, K. Su, K.S. Tan, J.F. White, J.A.M. Ramshaw, C. Lo, A. Rosamilia, J.A. Werkmeister, C.E. Gargett, Human endometrial mesenchymal stem cells modulate the tissue response and mechanical behavior of polyamide mesh implants for pelvic organ prolapse repair, Tissue Eng. Part A 20 (2014) 785–798.
[75] A.V. Vanikar, H.L. Trivedi, U.G. Thakkar, Stem cell therapy emerging as the key player in treating type 1 diabetes mellitus, Cytotherapy 18 (2016) 1077–1086.
[76] H. Vlassara, J. Uribarri, Advanced glycation end products (AGE) and diabetes: cause, effect, or both? Curr. Diab. Rep. 14 (2014) 453.
[77] H.-S. Wang, J.-F. Shyu, W.-S. Shen, H.-C. Hsu, T.-C. Chi, C.-P. Chen, S.-W. Huang, Y.-M. Shyr, K.-T. Tang, T.-H. Chen, Transplantation of insulin-producing cells derived from umbilical cord stromal mesenchymal stem cells to treat NOD mice, Cell Transplant. 20 (2011) 455–466.
[78] K.M. Wartchow, L. Rodrigues, L.Z. Suardi, B.C. Federhen, N.G. Selistre, C.-A. Gonçalves, P. Sesterheim, Short-term protocols to obtain insulin-producing cells from rat adipose tissue: signaling pathways and in vivo effect, Int. J. Mol. Sci. 20 (2019) 2458.
[79] J. Wu, L.-J. Yan, Streptozotocin-induced type 1 diabetes in rodents as a model for studying mitochondrial mechanisms of diabetic β cell glucotoxicity, Diabetes Metab. Syndr. Obes. Targets Ther. 8 (2015) 181–188.
[80] Y. Xin, X. Jiang, Y. Wang, X. Su, M. Sun, L. Zhang, Y. Tan, K.A. Wintergerst, Y. Li, Y. Li, Insulin-producing cells differentiated from human bone marrow Mesenchymal stem cells in vitro ameliorate Streptozotocin-induced diabetic hyperglycemia, PLoS One 11 (2016) e0145838.
[81] Z. Yang, K.K.W. Wang, Glial fibrillary acidic protein: from intermediate filament assembly and gliosis to neurobiomarker, Trends Neurosci. 38 (2015) 364–374.
[82] S.-Y. Yang, K.-C. Yang, S. Sumi, Effect of basic fibroblast growth factor on xenogeneic islets in subcutaneous transplantation-a murine model, Transplant. Proc. 51 (2019) 1458–1462.
[83] T. Zhang, X. Liu, Q. Li, J. Wang, W. Jia, X. Sun, Exacerbation of ischemia-induced amyloid-beta generation by diabetes is associated with autophagy activation in mice brain, Neurosci. Lett. 479 (2010) 215–220.
[84] W.-J. Zhang, Y.-F. Tan, J.T.Y. Yue, M. Vranic, J.M. Wojtowicz, Impairment of hippocampal neurogenesis in streptozotocin-treated diabetic rats, Acta Neurol. Scand. 117 (2008) 205–210.
[85] K. Zhao, H. Hao, J. Liu, C. Tong, Y. Cheng, Z. Xie, L. Zang, Y. Mu, W. Han, Bone marrow-derived mesenchymal stem cells ameliorate chronic high glucose-induced β-cell injury through modulation of autophagy, Cell Death Dis. 6 (2015) e1885.
[86] X.-Y. Zheng, Q.-Q. Wan, C.-Y. Zheng, H.-L. Zhou, X.-Y. Dong, Q.-S. Deng, H. Yao, Q. Fu, M. Gao, Z.-J. Yan, et al., Amniotic mesenchymal stem cells decrease Aβ deposition and improve memory in APP/PS1 transgenic mice, Neurochem. Res. 42 (2017) 2191–2207.
[87] Z. Zhou, Z. You, Mesenchymal stem cells alleviate LPS-induced acute lung injury in mice by MiR-142a-5p-controlled pulmonary endothelial cell autophagy, Cell. Physiol. Biochem. Int. J. Exp. Cell. Physiol. Biochem. Pharmacol. 38 (2016) 258–266.
[88] Y. Zhou, Y. Luo, J. Dai, Axonal and dendritic changes are associated with diabetic encephalopathy in rats: an important risk factor for Alzheimer's disease, J. Alzheimers Dis. JAD 34 (2013) 937–947.